Available online at www.sciencedirect.com
ScienceDirect
ELSEVIER
Global and Planetary Change xx (2006) xxx – xxx
GLOBAL AND PLANETARY CHANGE
www.elsevier.com/locate/gloplacha

Glacier inventory of the Gran Campo Nevado Ice Cap in the Southern Andes and glacier changes observed during recent decades

Christoph Schneider [a,*], Michael Schnirch [a], César Acuña [b], Gino Casassa [b], Rolf Kilian [c]

[a] *Institut für Physische Geographie, Universität Freiburg, Germany*
[b] *Centro de Estudios Cientificos, Valdivia, Chile*
[c] *Fachbereich Geowissenschaften, Universität Trier, Germany*

Abstract

The Gran Campo Nevado (GCN) forms an isolated ice cap on the Península Muñoz Gamero (PMG) located 200 km to the south of the Southern Patagonia Icefield (SPI). We present a glacier inventory of the GCN made up by 27 drainage basins (in total 199.5 km^2) and other small cirque and valley glaciers of the southern part of PMG (in total 53 km^2). The glacier inventory is based on a digital elevation model (DEM) and ortho-photos. Contour lines from maps, relief information derived from Landsat TM satellite imagery from 1986 and 2002 and stereoscopic data from aerial photos were combined in a knowledge-based scheme to obtain a DEM of the area. A digital ortho-photo map based on aerial photos from 1998 and several ortho-photos based on aerial photos from 1942 and 1984 could be produced from the initial DEM. A geographical information system (GIS) served to outline the extent of the present glaciation. All major glaciers of the GCN show a significant glacier retreat during the last 60 yr. Some of the outlet glaciers lost more than 20% of their total area during this period. Overall glacier retreat amounts to 2.8% of glacier length per decade and the glacier area loss is 2.4% per decade in the period from 1942 to 2002. We hypothesise that GCN glaciers may have reacted faster and more synchronously with the observed warming trend during recent decades when compared with the SPI.

Keywords: digital photogrammetry; geographical information systems (GIS); glacier inventory; glacier change; Patagonia

1. Introduction

The Gran Campo Nevado Ice Cap (GCN) is located at 53°S on the southern part of Península Muñoz Gamero (PMG), Chile (Fig. 1). The GCN forms the only major ice body between the Southern Patagonia Icefield and the Strait of Magallan. Until recently, the GCN has not been studied in detail. However, its almost unique location in a zone affected all year round by strong westerlies makes it a region of key interest in terms of glacier and climate change studies of the west-wind zone of the Southern Hemisphere. The aim of this study is to document the present extent of the glaciated area of the PMG and to quantify the historical (last 60 yr) glacier retreat. Since the GCN represents only a small ice cap, it is assumed that the response time of the GCN to climate change is much shorter than e.g. the response time of glacier

* Corresponding author. Tel.: +49 241 80 96048; fax: +49 241 80 92157.
E-mail address: christoph.schneider@geo.rwth-aachen.de (C. Schneider).

0921-8181/$ - see front matter © 2006 Published by Elsevier B.V.
doi:10.1016/j.gloplacha.2006.11.023

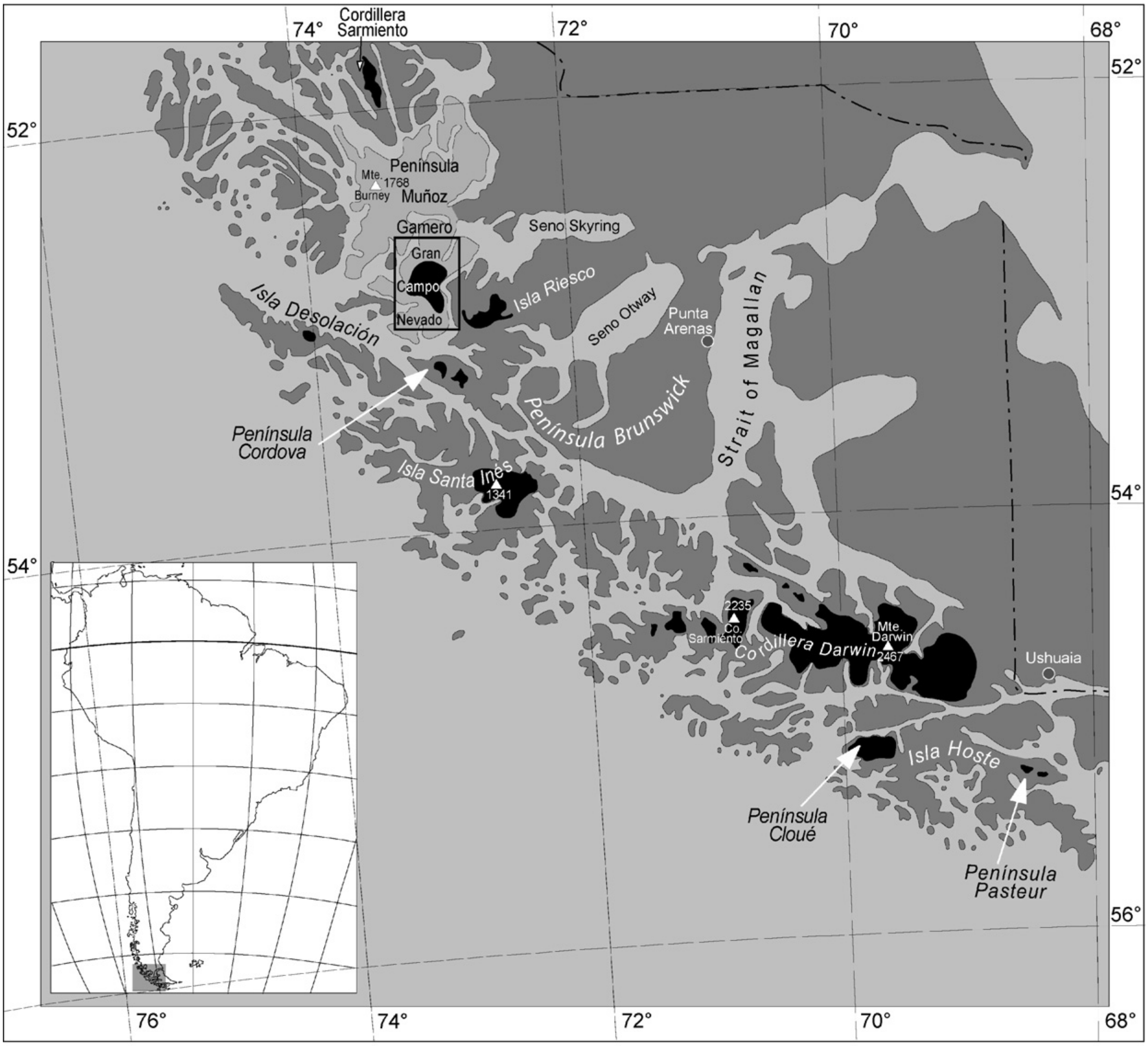

Cartographie: Klaus-Dieter Lickert, Freiburg

Fig. 1. Location of glaciated areas, denoted in black in southernmost South America. The Península Muñoz Gamero is shown in pale grey. The area of investigation covered by Fig. 4 is denoted by a black rectangle.

tongues at the Southern Patagonia Icefield (SPI). Furthermore, humid and temperate climate conditions lead to a large mass turnover. Therefore, we assume that the GCN having only a small mean elevation of 880 m asl shows very high sensitivity to climate change according to considerations by Oerlemans and Reichert (2000).

Although absolute altitudes are moderate south of the Southern Patagonia Icefield (SPI) along the Andes of southernmost South America there are a number of smaller scale glaciated areas located between 52°S and the southern tip of the continent (Fig. 1). The snow line is lower down further south because of generally lower temperatures. South of the Strait of Magallan there are major ice entities on Isla Hoste and on Isla Santa Inés (Casassa, 1995). Furthermore, a large icefield of approx. 2300 km^2 is located in the Cordillera Darwin on Tierra del Fuego (Lliboutry, 1998). North of the Strait of Magallan glaciation is confined to Cordillera Sarmiento directly south of SPI, and to Isla Riesco and PMG (Fig. 1). According to Casassa (1995) all of these glaciated areas in southernmost South America lack a detailed glacier inventory. Glaciation on Isla Riesco between Seno Otway and Seno Skyring merely consists of three small ice caps and a number of valley or cirque glaciers with a combined surface area of approximately 215 km^2. These have lately been inventoried by Casassa

Please cite this article as: Schneider, C. et al. Glacier inventory of the Gran Campo Nevado Ice Cap in the Southern Andes and glacier changes observed during recent decades. Global and Planetary Change (2006), doi:10.1016/j.gloplacha.2006.11.023

et al. (2002a). In this paper we present glacier inventory on the southern part of the PMG.

The PMG represents the eastern part of the zone of canals and fjords on the Pacific coast of Patagonia along 73°W and between 52°S and 53°S (Fig. 1). Both parts of the PMG are linked by a narrow land bridge to the mainland just north of Seno Skyring (Fig. 1). On the northern part of PMG a small ice cap is found in the northwest on Monte Burney Vulcano with an altitude of 1768 m asl. The southern part of PMG includes in its centre the GCN and a few small cirque and hanging glaciers. Lliboutry (1956) estimates the glaciated area on PMG to be 200 km^2. At the summit of Monte Pyramide the GCN reaches approximately 1740 m asl. The elevated plateau-like part of the ice cap is located at about 1200 m asl. The ice descends over many séracs down into outlet glaciers. Some of the outlet glaciers calve into proglacial lakes only slightly above sea level or into fjords. Paskoff (1996) uses the GCN as an example of an ice cap with radial outlet glaciers. The GCN may be considered as the moderate remnants of the extensive glaciation during the last glacial maximum covering large areas especially to the east of PMG including Seno Skyring (Caldenius, 1932; Mercer, 1970; Mercer, 1976; Kilian et al., 2003; Kilian et al., 2004-this issue).

Climate conditions can be described as extremely windy, moderately cool and very humid according to Miller (1976) and Zamora and Santana (1979). The regional climate at the GCN has a mean annual air temperature of +5.7 °C and 6500 mm of annual precipitation at sea level and has been investigated in detail by Schneider et al. (2003). High precipitation occurs during the whole year with a moderate maximum of precipitation falling during austral summer. Daily and seasonal temperature amplitudes are very low due to the vicinity of the Pacific with an amplitude between the warmest and coldest months of only 7.4 °C. The increase in precipitation at higher altitudes is considerable with more than 10,000 mm water equivalent of annual solid precipitation falling at higher altitudes on the GCN Ice Cap (Schneider et al., 2003).

Aerial photos dating back to the early 1940's indicate a general glacier retreat in most places in southernmost South America. Glacier retreat is larger at the SPI than at the Northern Patagonia Icefield (NPI) (Warren and Aniya, 1999) This may be attributed to the fact that the warming trend observed in Patagonia in the 20th century seems to be larger further south (Rosenblüth et al., 1997; Villalba et al., 2003). This paper investigates glacier change at the GCN Ice Cap since 1942 based on remote sensing imagery of different origin.

2. Data and methods

2.1. General approach

The construction of a glacier database for the GCN and the investigation of glacier changes were accomplished using data sets obtained by remote sensing and Geographical Information System (GIS) technology. The primary data sources include ortho-rectified aerial photos and Landsat Thematic Mapper (TM) images. A prerequisite for the production of ortho images from standard aerial photos is a digital elevation model (DEM). However, the available data did not allow for an automatic, digital photogrammetric calculation of the DEM. Therefore, the DEM was derived from digitised contour lines from topographic maps within GIS software. Spatial interpolation of altitudes was achieved using triangular irregular network(ing) (TIN) which allowed for the integration of information from different sources. The DEM was used to ortho-rectify aerial imagery taken in 1984 and in 1942.

The complete work flow is presented in Fig. 2. Basic photogrammetric processing was partly carried out at the Department of Geography, University of Düsseldorf (Germany) using the software tool *BLUH* from the University of Hannover, Department of Photogrammetry and Geoinformation. For further photogrammetric analysis and digital generation of ortho images, the software package *LISA FOTO* (Linder, 2001) was used. Satellite imagery was geo-referenced using *ERDAS Imagine* and *IDRISI* (Eastman 1999) software. To mosaicortho images of GCN, the production of the glacier inventory and analysis of glacier changes *ArcView GIS* (ESRI Co.) was used.

2.2. Data sets

Two topographic map sheets with a scale of 1:100,000 from the Instituto Geografico Militar de Chile, Santiago de Chile (IGM), "*Golfo Xaultegua*" and "*Lago Muñoz Gamero*" formed the topographic basis. These maps are referenced to the UTM co-ordinate system with the geodetic date "*South America 1969*". They are based on the aerial survey made in 1984. From the UTM co-ordinate grid of the maps 20 control points were digitised from each scanned map. The scans were geo-referenced using a second order transfer function based on the 20 control points. The resulting mean positional error of all control points derived from the second order fit amounts to ±9 m.

Three different data sets of aerial photos taken in 1942, 1984 and 1998 were available, all of these

Please cite this article as: Schneider, C. et al. Glacier inventory of the Gran Campo Nevado Ice Cap in the Southern Andes and glacier changes observed during recent decades. Global and Planetary Change (2006), doi:10.1016/j.gloplacha.2006.11.023

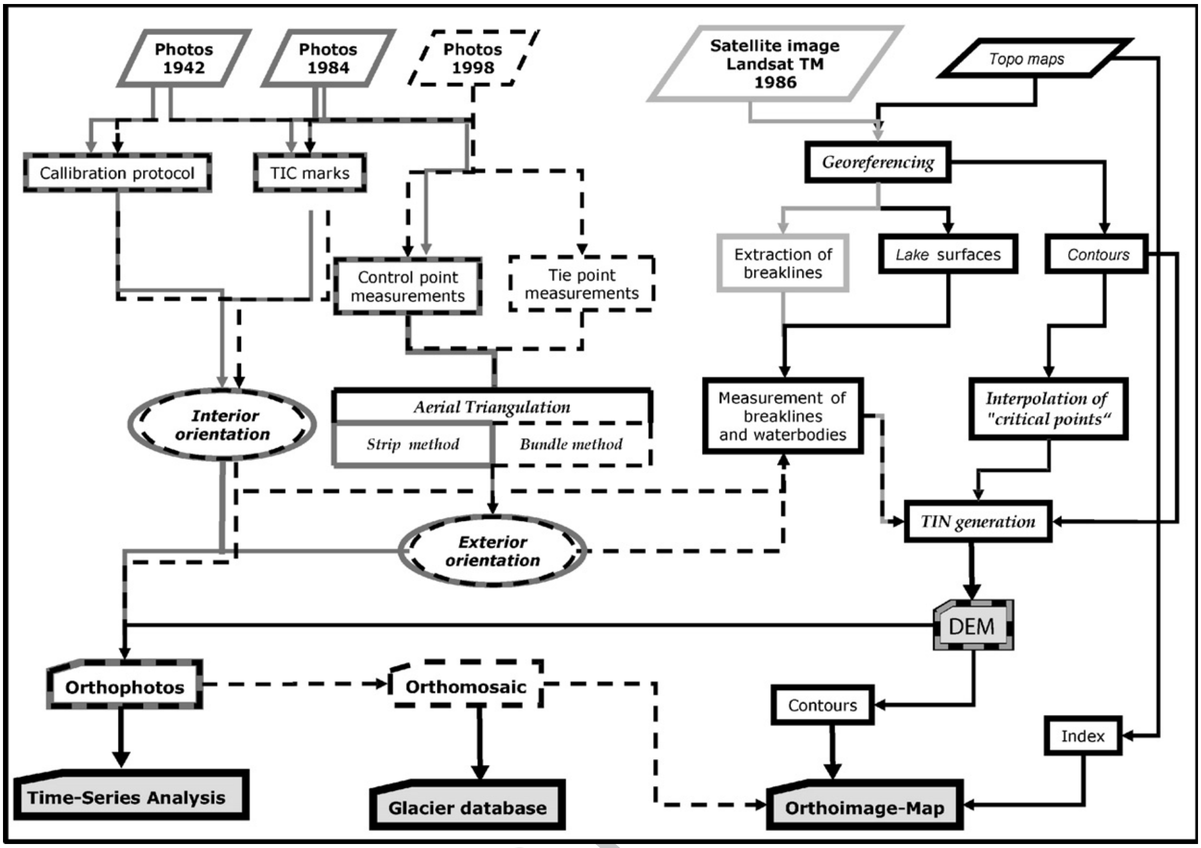

Fig. 2. Flow chart of the processing chain from aerial photography, satellite imagery and topographical maps to glacier inventory and glacier changes.

originating from the IGM. Imagery from 1942 was acquired by the United States of America Air Force. These series were not acquired for quantitative photogrammetric analysis. Pictures include vertical and oblique images along single flight lines and do not provide a possibility for the production of stereoscopic models and digital terrain models (DEM). The data are of low photogrammetric accuracy. No camera calibration protocol could be provided for these series of images. Aerial photos from 1984 and 1998 were acquired by the *Servicio Aerofotogramétrico de la Fuerza Aérea de Chile* (SAF). Based on the image series of 1984 the topographical maps were produced by the IGM. Although the general contrast in these images is very good, there are some shadowy areas and some snowy glacier surfaces that could not be photogrammetrically measured due to low contrast, which is indicated on the topographical maps. Aerial images from 1998 can only partly be used for photogrammetric processing due to the extreme contrast between shadows and snow and glacier surfaces. Of all the available images only the 1998 series completely covers the area of interest (Fig. 3) at a mean scale of 1:79,000. Earlier imagery was taken at lower altitudes and therefore shows more details. The relation of image base to altitude is very low due to the high altitude of the flight path of the aircraft, which causes extra deficiencies in the photogrammetric measurements of altitudes within the photogrammetric model (Schwiedefsky and Ackermann, 1976; Linder, 2001).

The inner orientation of the 1984 and 1998 image series was calculated based on the available camera calibration protocols. Inner orientation of the 1942 images had to be estimated using a software tool integrated into *LISA FOTO* software (Linder, 2001). Missing documentation and missing collimation markers of these images led to general lower precision.

Ground control points for the computation of the exterior orientation of the 1998 image series were derived from the topographic maps. The co-ordinates of the ground control points were taken directly from the digitised maps resulting in positional errors of ±30 m. However, this mean positional error itself is an estimation since no extra ground control points for external verification were available. Twelve stereoscopic image pairs of the 1998 images were computed with software

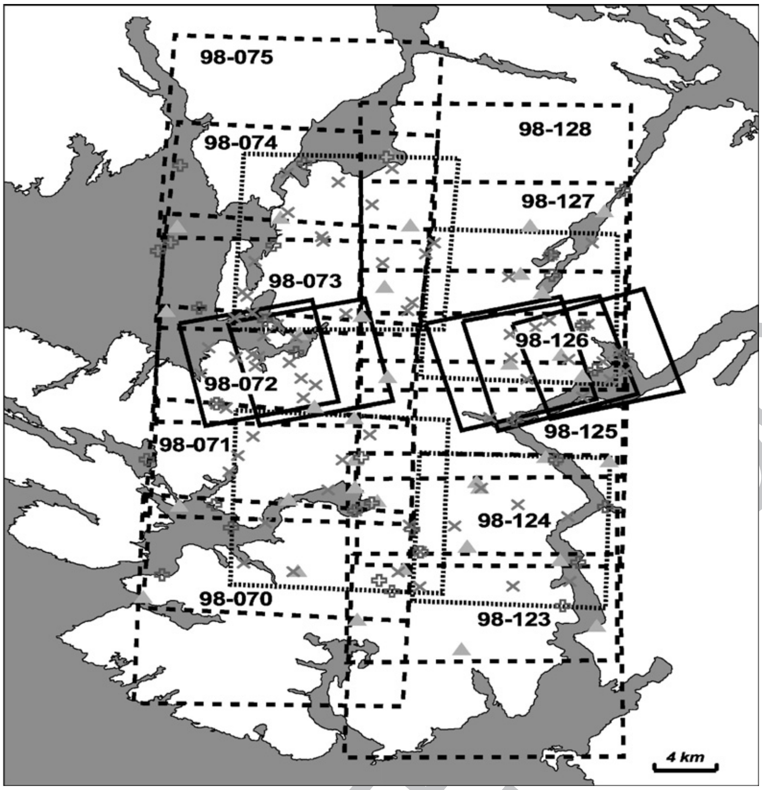

Fig. 3. Location of ground control points (open crosses) and tie points (triangles) of the bundle of images from 1998 (broken lines), and location of ortho images from 1942 (dotted lines) and 1984 (straight lines) and relevant ground control points for geo-referencing of the images from 1942 and 1984 (tilted crosses).

BLUH at the Department of Geography, University of Düsseldorf using the method of bundle adjustment in order to obtain the exterior orientation of the images. The parameters of exterior orientation of the 1942 and 1984 images were obtained using the method of spatial resection. Control points for this step were photogrammetrically measured within the stereoscopic model derived from the 1998 image series. Therefore, an adequate number of ground control points with *x*-, *y*- and *z*-coordinates were obtained to ensure a reliable relative orientation of all images to each other (Figs. 2,3).

Two Landsat TM satellite images were used to delineate glacier extent. The first image from the Landsat TM 5 sensor dates from 6th October 1986 with a maximum ground resolution of 30 m. The second was acquired by the Landsat 8, ETM+ satellite on 16th March 2002. This image offers a panchromatic band with 15 m ground pixel resolution. Using ground control points and a second order polynomial function both satellite images were geo-referenced to the geometry of the 1998 ortho-rectified aerial imagery mosaic. Mean positional error calculated from all ground control points is about 1 pixel (exactly ±32 m) after the geo-referencing with a maximum deviation of less than 2 pixels (±57 m).

2.3. Digital elevation model

Generation of a DEM from different information sources has been used by many authors (e.g. Linder, 1994; Eklundh and Martensson, 1995; Martinoni and Bernhard, 1998). In the case of GCN, the interpolation of contour lines (e.g. Schneider, 1998) was combined with single photogrammetric point measurements and breaklines derived from remote sensing imagery. (see e.g. Gruber and Kriz, 1998).

Altitude information from contour lines, breaklines and single altitude points was extracted from the scanned topographical maps by digitisation. Major water bodies were digitised and set to the altitude of the lake or to sea level along the coast line. Altitudes of 103 single points were used to check the accuracy of the DEM after interpolation. Information on relief ridges (breaklines) was partly extracted from the satellite image taken in 1986 in areas where low contrast did not allow these forms to be derived from the aerial photos. This additional information does not include explicit altitude information but only geomorphological shape. Therefore, photogrammetric measuring of individual points within the aerial photogrammetric model based on the imagery from 1998 was necessary to include this kind of information in the DEM. Morphological reasonable estimation of altitude information along breaklines was estimated using an algorithm based on so-called "*Critical Points*" (Zhu et al., 1999), within IDRISI software (Eastman, 1999).

All different information on altitudes available from various sources was integrated into a TIN using *ArcView 3D Analyst* software. This step involved the following primary data sources:

(1) Altitude contour lines with *z*-values from the maps,
(2) "*critical points*" along of breaklines, generated by *IDRISI 32* with TIN using the option "*Remove Bridge and Tunnel Edges*",
(3) polygons of lakes and sea surfaces (altitude of lakes was measured by photogrammetric restitution),
(4) 94 single points measured by photogrammetric restitution along breaklines on the GCN Ice Cap.

Primary data covers an area of 2160 km^2. The DEM includes most of the southern part of the PMG and contains all glaciated areas. The TIN was converted to a raster data set with 5 m ground resolution. Relevant parameters of the DEM are summarised in Table 1.

The interpolation algorithm based on the approach using critical points underestimates the true altitude along ridges. However, there is considerable improvement in terms of morphological accuracy (Schnirch, 2001).

Different sources of errors must be considered:

(1) errors inherent in the primary data sources of the topographic maps, the scanning and geo-coding of scanned maps,
(2) errors occurring during the process of digitising contour lines from the scanned maps,
(3) errors resulting from the interpolation process.

Table 1
Pertinent data of the DEM Gran Campo Nevado and its TIN

Parameter	Value
Altitude range	0–1699 m
Vertical precision	~35 m
Relative horizontal precision	~9 m
Number of knots	291,615
Number of triangular irregular areas	583,199

In order to estimate the error of the derived DEM the root mean square error (rms) of the deviations (h_i) between the exact altitude as derived from the maps and altitude obtained from the DEM of 103 altitude points from summits and ridges was calculated according to Bartelme (2000):

$$\mathrm{rms} = \sqrt{\sum_{i=1}^{n} \frac{1}{n} h_i^2}. \qquad (1)$$

The mean error resulting from this procedure is ± 35.4 m. Parts of the accumulation area of the ice cap, where only little topographic information was available, could only be roughly estimated because no detailed information was available — neither from the maps nor from photogrammetric restitution. Therefore, the exact topography of the ice cap summit area is not known and the DEM of the summit area of GCN reveals meso-scale morphological structure only.

2.4. Generation of an ortho image map

The generation of ortho images was accomplished with software *LISA FOTO* using a DEM and the orientation parameters of the aerial photos. Subsequently, module *mosaic* within *LISA* allows for the combination of all individual ortho images to produce a single ortho image mosaic. The 1998 image series was rectified accordingly using the DEM. However, the altitude information mainly dates from 1984. Therefore, some deviation has to be considered, especially on the glacier surfaces. Ortho-rectification was carried out separately using the procedure of spatial resecting for all images from the different series of 1942 and 1984 without orientation parameters from bundle adjustment.

After rectification, the spatial resolution of all imagery was set to 5 m. The ortho image mosaic, glacier outlines and glacier numbering are presented in Fig. 4.

3. Results

3.1. Glacier inventory of the 'Península Muñoz Gamero South'

The mosaic of ortho images of the image series taken in 1998 (Fig. 4) was used to delineate glacier surfaces on the southern part of PMG. Imagery dates from 21st February indicating that the analysis is influenced only

Please cite this article as: Schneider, C. et al. Glacier inventory of the Gran Campo Nevado Ice Cap in the Southern Andes and glacier changes observed during recent decades. Global and Planetary Change (2006), doi:10.1016/j.gloplacha.2006.11.023

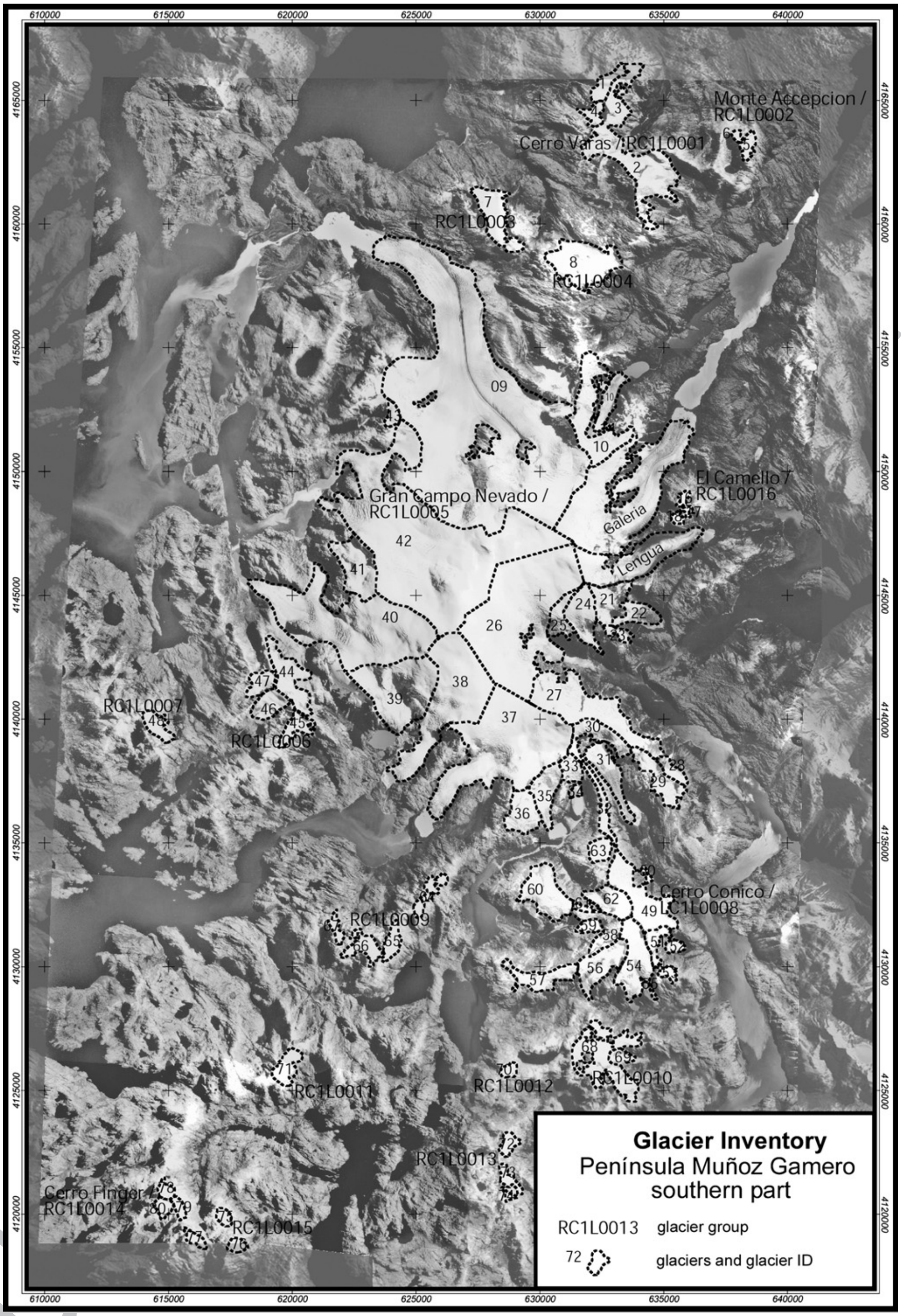

Fig. 4. Ortho image map of the southern part of Península Muñoz Gamero and glacier inventory of the Gran Campo Nevado an adjacent small cirque glaciers at 53°S.

by few temporary snow fields. It is assumed that all major areas covered by snow are located on glaciers or comprise at least large firn fields. The analysis underestimates sloped surfaces due to the vertical projection. In parts, delineation of glaciers was difficult due to coverage with surface moraines. The error is estimated

Please cite this article as: Schneider, C. et al. Glacier inventory of the Gran Campo Nevado Ice Cap in the Southern Andes and glacier changes observed during recent decades. Global and Planetary Change (2006), doi:10.1016/j.gloplacha.2006.11.023

t2.1 Table 2

t2.2 Position, area, width, length, exposition, and altitude range of glaciers of Península Muñoz Gamero, southern part

t2.3	Glacier group	Glacier name	WGMS numbers	Northing	Easting	Area	Mean width	Mean length	Exposition	Max. elevation	Min. elevation
t2.4	Varas/RC1L0001	GCN01	RC1G00101001	4165743	632820	0.87	0.44	1.67		1098	845
t2.5		GCN02	RC1G00101002	4163153	632560	6.91	0.58	6.16	E	1110	428
t2.6		GCN03	RC1G00101003	4165378	633315	0.10	0.2	0.45	E	792	489
t2.7		GCN04	RC1G00101004	4164478	632090	0.57	0.44	1.17	W	1034	746
t2.8	M. Acepción/RC1L0002	GCN05	RC1G00101005	4163203	638455	0.49	0.40	1.09	E	1010	677
t2.9		GCN06	RC1G00101006	4163568	638020	0.15	0.30	0.45	NE	1010	812
t2.10	RC1L0003	GCN07	RC1G00101007	4160218	628285	2.36	0.62	3.09	NE	1050	490
t2.11	RC1L0004	GCN08	RC1G00101008	4158298	631585	3.95	1.25	1.79		910	554
t2.12	Gran Campo Nevado/RC1L0005	GCN09	RC1G00101009	4153503	627670	51.46	3.45	12.16	NW	1625	101
t2.13		GCN10	RC1G00101010	4152533	631855	5.80	0.47	4.92	E	1420	96
t2.14		Galería	RC1G00101016	4149518	634445	13.65	1.17	6.00	NE	1682	0
t2.15		Lengua	RC1G00101019	4146678	634845	5.32	0.85	4.99	E	1678	98
t2.16		GCN21	RC1G00101020	4144703	632855	1.94	0.81	1.77	SW	1402	273
t2.17		GCN22	RC1G00101021	4144268	633970	1.23	0.55	1.63	E	777	105
t2.18		GCN23	RC1G00101022	4143463	633200	0.43	0.36	1.19	E	1066	547
t2.19		GCN24	RC1G00101023	4144828	631805	2.23	0.52	3.07	S	1678	225
t2.20		GCN25	RC1G00101024	4144378	630720	1.19	0.34	1.56	S	1414	429
t2.21		GCN26	RC1G00101025	4143908	629200	17.25	2.25	6.52	SW	1671	0
t2.22		GCN27	RC1G00101026	4140238	632295	6.37	0.96	5.91	NE	1534	245
t2.23		GCN28	RC1G00101027	4137943	635375	0.64	0.40	1.43	NE	1037	446
t2.24		GCN29	RC1G00101028	4137663	634840	1.98	0.64	2.76	S	1042	494
t2.25		GCN30	RC1G00101029	4139173	632430	1.87	0.50	3.85	SE	1530	465
t2.26		GCN31	RC1G00101030	4137463	632845	2.10	0.53	3.54	S	734	189
t2.27		GCN32	RC1G00101031	4136573	632620	0.95	0.23	3.49	E	915	511
t2.28		GCN33	RC1G00101032	4138068	631275	0.78	0.66	1.00	SE	1416	603
t2.29		GCN34	RC1G00101033	4137133	631465	0.21	0.27	0.36	SE	645	401
t2.30		GCN35	RC1G00101034	4136913	630270	1.91	0.61	2.34	S	1363	314
t2.31		GCN36	RC1G00101035	4136353	629350	1.88	1.06	1.42	S	1202	582
t2.32		GCN37	RC1G00101036	4138718	628420	14.39	1.65	5.37	S	1522	50
t2.33		GCN38	RC1G00101037	4140513	626010	9.47	1.23	4.30	SW	1626	58
t2.34		GCN39	RC1G00101038	4141013	624000	6.92	1.71	2.61	S	1578	185
t2.35		GCN40	RC1G00101039	4144168	622090	15.06	1.58	5.58	W	1606	118
t2.36		GCN41	RC1G00101040	4146128	622455	3.10	1.20	2.18	NW	1326	451
t2.37		GCN42	RC1G00101041	4146836	625377	30.91	1.99	7.86	NW	1654	0
t2.38		GCN43	RC1G00101042	4152393	624035	0.44	0.36	0.80	W	1067	768
t2.39	RC1L0006	GCN44	RC1G00101046	4141768	619770	2.46	0.58	2.29	NE	912	513
t2.40		GCN45	RC1G00101047	4139638	620160	0.96	0.53	0.91	SE	927	429
t2.41		GCN46	RC1G00101048	4140598	619070	1.28	0.81	1.18	SW	884	474
t2.42		GCN47	RC1G00101049	4141458	618710	0.87	0.59	1.23	SW	811	610
t2.43	RC1L0007	GCN48	RC1G00101050	4139728	614545	0.88	0.57	1.43	NE	805	500
t2.44	Cerro Cónico/RC1L0008	GCN49	RC1G00101051	4133073	634200	3.62	0.84	3.67	NE	1215	64
t2.45		GCN50	RC1G00101052	4133713	634375	0.14	0.11	0.60	E	375	61
t2.46		GCN51	RC1G00101053	4130818	634575	0.79	0.33	1.42	E	1112	191
t2.47		GCN52	RC1G00101054	4130798	622790	0.32	0.38	0.74	E	293	107
t2.48		GCN53	RC1G00101055	4129733	635160	0.34	0.35	0.67	SE	856	516
t2.49		GCN54	RC1G00101056	4130343	633830	3.06	0.88	2.72	S	1238	147
t2.50		GCN55	RC1G00101057	4129038	634620	0.08	0.11	0.64	S	538	200
t2.51		GCN56	RC1G00101058	4129928	632570	2.33	1.37	2.33	S	1167	292
t2.52		GCN57	RC1G00101059	4129668	630030	1.75	0.49	3.17	S	1029	434
t2.53		GCN58	RC1G00101060	4131418	632955	1.58	0.44	3.15	SW	1214	737
t2.54		GCN59	RC1G00101061	4131678	632050	0.45	0.34	0.89	W	807	511
t2.55		GCN60	RC1G00101062	4133043	630210	2.90	1.14	2.18		1107	552
t2.56		GCN61	RC1G00101063	4132468	631930	0.26	0.19	0.90	NW	942	687
t2.57		GCN62	RC1G00101064	4132603	632745	1.67	0.75	1.77	W	1220	524
t2.58		GCN63	RC1G00101065	4134723	632475	0.75	0.65	0.95	NW	991	719
t2.59	RC1L0009	GCN64	RC1G00101066	4132908	625590	0.77	0.28	1.88	SE	881	527
t2.60		GCN65	RC1G00101067	4131068	624005	0.74	0.81	1.33	SE	910	547

Please cite this article as: Schneider, C. et al. Glacier inventory of the Gran Campo Nevado Ice Cap in the Southern Andes and glacier changes observed during recent decades. Global and Planetary Change (2006), doi:10.1016/j.gloplacha.2006.11.023

Table 2 (*continued*)

Glacier group	Glacier name	WGMS numbers	Northing	Easting	Area	Mean width	Mean length	Exposition	Max. elevation	Min. elevation
RC1L0009	GCN66	RC1G00101068	4130838	635510	1.09	0.40	1.54	SW	933	600
	GCN67	RC1G00101069	4131628	621760	0.38	0.26	1.14	NE	856	623
RC1L0010	GCN68	RC1G00101070	4126223	632750	4.10	0.77	2.39	E	1009	522
	GCN69	RC1G00101071	4126383	633355	0.49	0.43	0.99	E	826	302
RC1L0011	GCN71	RC1G00101073	4125988	619775	1.06	0.58	1.40	SE	853	373
RC1L0012	GCN70	RC1G00101072	4125873	628760	0.30	0.39	0.64	S	906	676
RC1L0013	GCN72	RC1G00101074	4122848	628795	0.49	0.48	0.89	E	858	503
	GCN73	RC1G00101075	4121448	628850	0.47	0.29	0.89	SE	804	454
	GCN74	RC1G00101076	4120833	628790	0.13	0.15	0.47	E	800	516
RC1L0014	GCN77	RC1G00101079	4119068	616035	0.36	0.28	1.00	E	948	628
	GCN78	RC1G00101080	4121058	614855	0.39	0.35	0.72		926	581
	GCN79	RC1G00101081	4120268	615345	0.32	0.34	0.95	E	931	679
	GCN80	RC1G00101082	4120283	614745	0.44	0.47	0.77	S	923	598
RC1L0015	GCN75	RC1G00101077	4119913	617210	0.34	0.42	0.72	E	898	645
	GCN76	RC1G00101078	4118788	617755	0.35	0.42	0.70	E	922	616
El Camello/RC1L0016	GCN16	RC1G00101043	4148938	635820	0.20	0.24	0.71	NE	984	633
	GCN17	RC1G00101044	4148408	635995	0.13	0.16	0.51	SE	1030	658
	GCN18	RC1G00101045	4148193	635600	0.19	0.25	0.36	S	1030	654

Areas and lengths are given in km or km^2. Altitudes are given in m. Glacier names are provisional.

to be less than 10% although no direct terrestrial survey was available for comparison.

Altogether 81 polygons were marked as glaciers resulting in a total area of 252.56 km^2. The largest individual area with almost 60 km^2 is made up by the plateau of the GCN Ice Cap. However, this area does not constitute an individual glacier but makes up the combined accumulation area of a variety of individual outlet glaciers. Therefore, this area was subdivided into the surrounding outlet glaciers using module *watershed* within *IDRISI* software according to surface topography (Eastman, 1999). This entails errors due to the fact that surface topography does not necessarily indicate flow direction of glaciers. Furthermore, the exact topography of the ice surface on the plateau in places is only very roughly known (see Section 2.3). These shortcomings result in straight glacier boundaries between glaciers on the plateau, which must be considered as artefacts. It is hoped to overcome these shortcomings in the near future by deriving exact topography and flow lines from radar interferometry.

Subsequently, some small glacier areas on the east side of the GCN Ice Cap were combined to form larger entities because these areas constitute the same drainage basin with separated accumulation and ablation areas which are connected by steep séracs (Glaciar Lengua, Glaciar Galería and Glaciar No. 10 in Fig. 4). After this procedure we obtained 75 glaciers organised into 16 glacier groups on the southern part of PMG. The largest glacier group consists of 27 individual glaciers on the GCN Ice Cap, which cover an overall surface area of 199.5 km^2.

Glacier boundaries are presented in Fig. 4 overlain on the ortho image mosaic. Glacier numbering was attributed according to WGMS standards (Haeberli, 1995, 1998; Haeberli et al., 2000). Pertinent data of each glacier polygon are given in Table 2 including provisional glacier names and numbers as submitted to WGMS. This inventory closes one of the major gaps within the glacier inventory of Chile (see Casassa, 1995; Casassa et al., 1998).

3.2. Frontal variations and glacier surface area changes at GCN

After rectification and geo-coding of all available aerial imagery taken in 1942, 1984, and 1998 and the satellite data obtained in 1986 and 2002, the time series of five layers allowed glacier change at single outlet glaciers of the GCN to be assessed. Within each layer glacier outlines of 10 glacier tongues were digitised. Changes in the position of the glacier fronts and area changes were calculated. The respective glacier tongues can be deduced from the numbering or naming of the glaciers given in Fig. 4. As an example Fig. 5 presents glacier front recession at Glaciar Noroeste (No. 09). Some of the glacier area changes were aggregated with neighbouring glacier tongues that constitute the same drainage basin (No. 40 and No. 41/42).

Fig. 6 presents relative glacier surface changes per decade. Surface area and glacier length changes are summarised in Tables 3 and 4. Relative changes refer to glacier length and glacier surface area at the beginning

Please cite this article as: Schneider, C. et al. Glacier inventory of the Gran Campo Nevado Ice Cap in the Southern Andes and glacier changes observed during recent decades. Global and Planetary Change (2006), doi:10.1016/j.gloplacha.2006.11.023

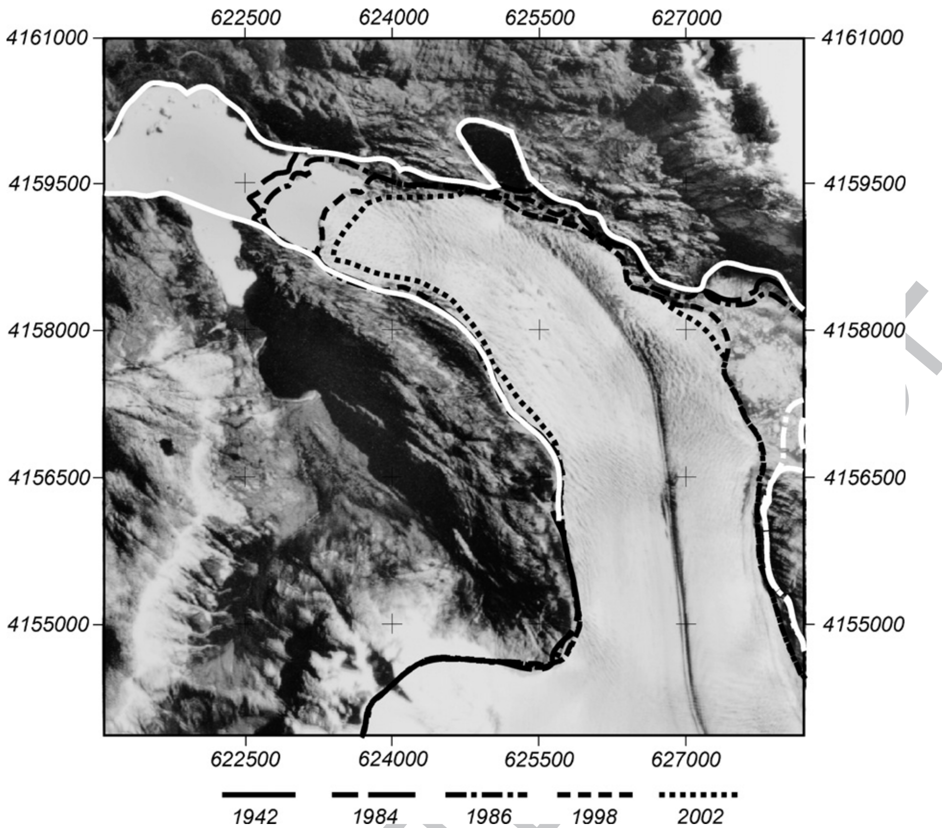

Fig. 5. Frontal position of the glacier tongue of Glaciar Noroeste (unofficial name), the largest outlet glacier of the Gran Campo Nevado, in 1942, 1984, 1986, 1998 and 2002. Aerial photo dating from/taken in 1998.

of the time interval considered. There is a considerable noise in the data and frontal variations and area changes greatly vary from period to period and from glacier basin to glacier basin without revealing a clear spatial pattern. An obvious relationship between the rate of retreat and the exposition, valley shape, or flow

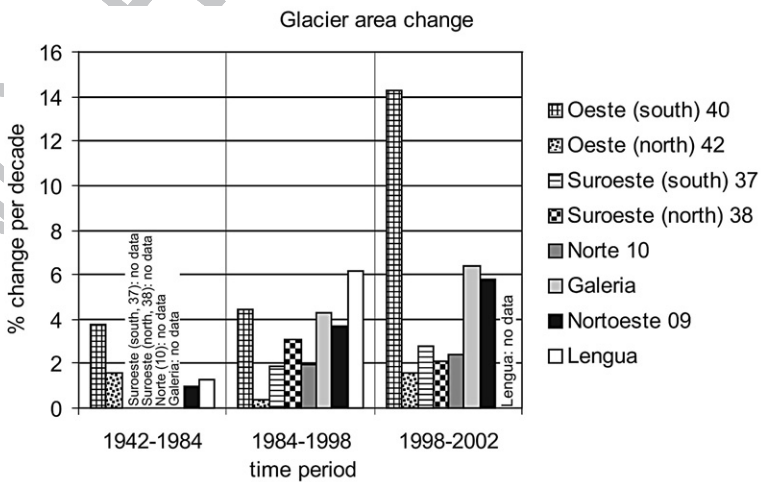

Fig. 6. Area changes in 8 outlet glaciers of the Gran Campo Nevado from 1942 to 2002.

Please cite this article as: Schneider, C. et al. Glacier inventory of the Gran Campo Nevado Ice Cap in the Southern Andes and glacier changes observed during recent decades. Global and Planetary Change (2006), doi:10.1016/j.gloplacha.2006.11.023

direction of the glacier tongues cannot be deduced. None of the investigated glaciers experiences glacier advance, but at some glaciers no change of the position of the glacier front was observed during at least some of the time. Only two glaciers (Oeste northern part/No. 42 and Norte/No. 10) do not show any changes between 1984/1986 and 2002. Many of the glaciers are calving into proglacial lakes or the sea. Rapid retreat is typical for this type of glacier because of the decay resulting from the contact with warm water after the glacier front loses contact with protecting ridges or frontal moraines. After the rapid retreat phase these glaciers sometimes remain at a new position until they are again pushed away from their new equilibrium state by further climate change (Meier and Post, 1987).

Most of the glaciers show an acceleration of retreat towards the end of the 20th century (Noroeste/No. 09, Oeste (south, left/No. 40), Oeste (south, right/No.40) and Galería), which indicates persistent negative mass balance (Haeberli et al., 1999). Maximum length changes amount to about −8% per decade. Two of the glaciers (Oeste (northern part/No. 42) and Noroeste/No. 09) have retreated by almost 2.5 km since 1942. Observed length changes range from −13% to −26% from 1942 to 2002. In the period from 1942 to 2002 a considerable retreat of 2.8% per decade was measured as the mean value of all investigated glacier tongues.

Mean observed retreat of glacier surface areas of 2.4% per decade is similar to the observed length changes. This indicates that the glaciers were not decaying but rather steadily retreating during the last 60 yr as a consequence of changing climate. Similar to the observed length changes since 1942 area losses vary widely from glacier to glacier with values ranging from 11% to 25% of the original surface area in 1942.

Table 3
Change in areas of 8 outlet glaciers of the Gran Campo Nevado Ice Cap 1942/1984–1998/2002

Glacier	Time period	Area loss (km^2)	Area loss (%)	Area loss per decade (%)
Oeste (south) 40	1942–2002	4.9	25.5	4.2
Oeste (north) 42	1942–2002	2.8	7.7	1.3
Suroeste (south) 37	1984–2002	0.6	3.7	2.1
Suroeste (north) 38	1984–2002	0.5	5.1	2.9
Noroeste 09	1942–2002	6.4	11.3	1.9
Norte 10	1984–2002	0.2	3.7	2.0
Galería	1984–2002	1.2	8.4	4.7
Lengua	1942–1998	0.7	13.4	2.4
All glaciers:	1942–2002	Weighted mean per decade: 2.4%		

Table 4
Change in lengths of 9 outlet glaciers of the Gran Campo Nevado Ice Cap 1942/1984–1998/2002

Glacier	Time period	Retreat (m)	Retreat (%)	Retreat per decade (%)
Oeste (south/right) 40	1942–2002	1639	18.9	3.2
Oeste (south/left) 40	1942–2002	1553	16.2	2.7
Oeste (north) 42	1942–2002	2447	20.6	3.4
Suroeste (south) 37	1984–2002	238	3.3	1.8
Suroeste (north) 38	1984–2002	380	5.5	3.1
Noroeste 09	1942–2002	2433	15.5	2.6
Norte 10	1984–2002	101	2.4	1.3
Galería	1984–2002	601	7.3	4.1
Lengua	1942–1998	617	9.0	1.6
All glaciers:	1942–2002	Weighted mean per decade: 2.8%		

Glaciers that show large rates of length changes do also lose a larger fraction of their surface area.

4. Discussion and conclusion

The glacier inventory and the construction of a glacier database including spatial data and a high resolution elevation model for each glacier of the southern part of the PMG provides important data for the national glacier inventory of Chile, the WGMS (Haeberli, 1995) and the Global Land Ice Measurement from Space (GLIMS) Project (www.glims.org). Furthermore, the database enables the development of distributed mass balance estimates for GCN Ice Cap in the near future. Therefore, this work represents an important step towards a glacier monitoring strategy in this very sensitive part of the world in terms of climate change and climate sensitivity (see also Schneider et al., 2004-this issue). Further work must consider the deficiencies of the DEM on the upper regions of the ice cap. Also, the delineation of single glacier drainage basins on the ice cap must be improved by observing flow lines on the ice cap. Both problems will be approached using the radar interferometry technique (Rignot et al., 2003).

In comparison to glacier changes during the 20th century observed at the SPI (see Section 1) absolute glacier retreat of the GCN Ice cap of about 1 km to 2 km at single glacier tongues does not seem to be moderate. The largest retreat of the glacier fronts at SPI is noted by Aniya et al. (1997) at the tongue of the calving Glaciar O'Higgins to the east of the SPI with a retreat of 14.6 km during the period from 1896 to 1995. Casassa et al. (2002b) estimate the mean change in ice thickness on the glacier tongues of SPI to be about −3.5 m/yr. At Glaciar Upsala (SPI) the reduction in the ice depth near

Please cite this article as: Schneider, C. et al. Glacier inventory of the Gran Campo Nevado Ice Cap in the Southern Andes and glacier changes observed during recent decades. Global and Planetary Change (2006), doi:10.1016/j.gloplacha.2006.11.023

the lower end of the glacier tongue between 1990 and 1993 add up to 11 m/yr (Naruse et al., 1997). Harrison and Winchester (2000) report a reduction in ice depth in the ablation zone of outlet glaciers to the east of the NPI by at least 30 m since 1980. However, during the 1990s only little glacier retreat was observed at the 21 outlet glaciers of the NPI based on aerial photos (Aniya, 2000).

Aniya (1999) estimates an area loss of approx. 270 km^2 and a volume loss of 825 km^3 ± 320 km^3 for the combined ice bodies of SPI and NPI since 1945. The total surface area of SPI and NPI is estimated to be 18,000 km^2 (Casassa et al., 2002b, Rivera et al., 2002). Using the value of surface area loss given by Aniya (1999) a relative decrease in surface area of SPI and NPI of 1.5% from 1945 to 1998 is calculated. In contrast, the combined surface area loss of the 8 largest drainage basins of the GCN is 14.4% over 60 yr from 1942 to 2002. Since 1984 these glaciers lost 9.2 km^2 of their surface area, which made up 4.6% of the total surface area of GCN in 1998. At some glacier tongues topographical constraints may have influenced the pattern of changes (Meier and Post, 1987), which is especially noticeable for the many calving glaciers of SPI and NPI (Rosenblüth et al., 1995; Warren and Aniya, 1999). Steady-state behaviour of some glaciers of the GCN over several years seems to be related to glacier bed topography within fjords and the formation of proglacial lakes. There is no indication that this would be related to positive mass balances during theses periods. In comparison to SPI and NPI, the high rate of ice surface loss of 2.5% per decade on the GCN indicates that, besides the observed warming trend (Rosenblüth et al., 1997), a decrease in mean precipitation during the 20th century must be considered.

Some glaciers of the SPI, e.g. Glaciar Pío XI, showed an increase in ice depth at the glacier tongue and some ice advance during recent years (Rivera et al., 1997a,b; Rivera and Casassa, 1999). Naruse et al. (1995) show that Glaciar Pío XI advanced by 8.5 km during 41 yr until 1990, probably as a consequence of surging (Rignot et al., 2003). In contrast, no glacier advances were observed on the southern part of the PMG. Aerial images taken in 1943, 1984 and 1993 indicate that glacier tongues to the south and to the west of the Cordillera Darwin on Tierra del Fuego show only little change. Glacier tongues with north and east orientation however experienced some retreat during this period (Holmlund and Fuenzalida, 1995). This indicates that in contrast to the glaciers of the GCN there has been no major ice retreat during the second half of the 20th century in the Cordillera Darwin. This may be attributed to differing climatic responses – especially precipitation changes – resulting from changes in the atmospheric circulation. Precipitation rates associated with different weather patterns in South Patagonia and Tierra del Fuego differ widely between west and east facing sides of the Andes (Schneider et al., 2003). Therefore, further research is needed to more clearly reveal the spatial and temporal pattern of precipitation in southernmost Patagonia and on Tierra del Fuego.

Using a formula provided by Jóhannesson et al. (1989) the response time (rt) of a glacier to climate change can be calculated from the ablation rate (b_t) and the glacier depth (h) at the glacier terminus to be

$$\mathrm{rt} = \frac{h}{b_t}. \tag{2}$$

Assuming glacier depths between 50 m and 300 m at the glacier terminus of the various outlet glaciers of the GCN we obtain response times ranging from 5 to 25 yr because of the high ablation rate at the GCN of about 12 m/a at sea level. This indicates that glacier changes during recent decades clearly reflect climate variations during the second half of the 20th century. Since the response times of the glaciers of the SPI must be much longer – in the order of decades – we may conclude that glacier reduction at the SPI will accelerate during coming decades.

Acknowledgements

The authors wish to thank Dr. W. Linder and Prof. E. Jordan, Dep. of Geography, Univ. of Düsseldorf for the provision of software and for their support with bundle block adjustment of aerial photos taken in 1998. This study was undertaken funded by grant No. Schn 680 1/1 of the German Research Society (Deutsche Forschungsgemeinschaft (DFG)).

References

Aniya, M., 1999. Recent glacier variations of the Patagónicos, South America, and their contribution to sea-level change. Arctic, Antarctic and Alpine Research 31, 165–173.

Aniya, M., 2000. Glacier variations of Hielo Patagonico Norte, Chilean Patagonia, since 1944/45, with special reference to variations between 1995/96 and 1999/2000. Bulletin of Glaciological Research 18, 55–63.

Aniya, M., Sato, H., Naruse, R., Skvarca, P., Casassa, G., 1997. Recent glacier variations in the Southern Patagonia Icefield, South America. Arctic and Alpine Research 29, 1–12.

Bartelme, N., 2000. Geoinformatik - Modelle, Strukturen, Funktionen. Springer, Berlin.

Caldenius, C.C., 1932. Las glaciaciones cuaternarios en la Patagonia y Tierra del Fuego. Geografiska Annaler 14, 1–164.

Casassa, G., 1995. Glacier inventory in Chile: current status and recent glacier variations. Annals of Glaciology 21, 317–322.

Casassa, G., Espizua, L.E., Francou, B., Ribstein, P., Ames, A., Alean, J., 1998. Glaciers in South America. In: Haeberli, W., Hoelzle, M., Suter, S. (Eds.), Into the Second Century of Worldwide Glacier Monitoring: Prospects and Strategies. UNESCO Publishing, Paris, pp. 125–146.

Casassa, G., Smith, K., Rivera, A., Araos, J., Schnirch, M., Schneider, C., 2002a. Inventory of glaciers in Isla Riesco, Patagonia, Chile, based on aerial photography and satellite imagery. Annals of Glaciology 34, 373–378.

Casassa, G., Rivera, A., Aniya, M., Naruse, R., 2002b. Current knowledge of the Southern Patagonia Icefield. In: Casassa, G., Sepulveda, F.V., Sinclair, R.M. (Eds.), The Patagonian Icefields. A unique natural laboratory for environmental and climate change studies, New York, pp. 67–82.

Eastman, J.R., 1999. Guide to GIS and image processing, Volume 2. IDRISI 32 User Guide, Worcester.

Eklundh, L., Martensson, U., 1995. Rapid generation of digital elevation models from topographic maps. International Journal of Geographical Information Systems 9, 329–340.

Gruber, D., Kriz, K., 1998. DGM-Optimierung als Basis für geomorphologische Fragestellungen. In: Kriz, K. (Ed.), Hochgebirgskartographie/Silvretta '98. Wiener Schriften zur Geographie und Kartographie, vol. 11, pp. 76–80.

Haeberli, W., 1995. Glacier fluctuations and climate change detections — operational elements of a worldwide monitoring strategy. World Meteorological Organisation Bulletin 44, 23–31.

Haeberli, W., 1998. Historical evolution and operational aspects of worldwide glacier monitoring. In: Haeberli, W., Hoelzle, M., Suter, S. (Eds.), Into the Second Century of World Glacier Monitoring — Prospects and Strategies. UNESCO publishing, Paris, pp. 35–51.

Haeberli, W., Frauenfelder, R., Hoelzle, M., Maisch, M., 1999. On rates and acceleration trends of global glacier mass changes. Geografiska Annaler 81A, 585–591.

Haeberli, W., Cihlar, J., Barry, R.G., 2000. Glacier monitoring within the global climate observing system. Annals of Glaciology 31, 241–246.

Harrison, S., Winchester, V., 2000. Nineteenth- and twentieth-century glacier fluctuations and climatic implications in the Acro and Colonia Valleys, Hielo Patagonico Norte, Chile. Arctic, Antarctic and Alpine Research 32, 55–63.

Holmlund, P., Fuenzalida, H., 1995. Anomalous glacier responses to 20th century climatic changes in Darwin Cordillera, southern Chile. Journal of Glaciology 41, 465–473.

Jóhannesson, T., Raymond, C., Waddington, E., 1989. Time-scale for adjustment of glaciers to changes in mass balance. Journal of Glaciology 35, 355–369.

Kilian, R., Fesq-Martin, M., Schneider, C., Biester, H., Casassa, G., Arevalo, M., Wendt, G., Behrmann, J., 2003. Late glacial ice retreat in the southernmost Andes: sedimentological and palynological implications. 10. Congreso Geologico Chileno. Publikation auf CD, Concepcion, p. 5S. 06.-10.10.2003.

Kilian, R., Schneider, C., Koch, J., Fesq-Martin, M., Biester, H., Casassa, G., Arévalo, M., Wendt, G., Baeza, O., Behrmann, J. 2004. Paleoecological constraints on late glacial to Holocene ice retreat in the Southern Andes (53°S). this issue of Global and Planetary change.

Linder, W., 1994. Interpolation und Auswertung digitaler Geländemodelle mit Methoden der digitalen Bildverarbeitung. Wissenschaftliche Arbeiten der Fachrichtung Vermessungswesen der Universität Hannover, vol. 198. Hannover.

Linder, W., 2001. Handbuch zu LISA-FOTO, Version 2.2. Geographisches Institut der Universität Düsseldorf, Düsseldorf.

Lliboutry, L., 1956. Nieves y glaciares de Chile. Santiago de Chile.

Lliboutry, L., 1998. Glaciers of the wet Andes. In: Williams, R.S., Ferrigno, J. (Eds.), Glaciers of South America, U.S. Geological Survey Professional Paper, 1386–1. U.S.G.S., Washington, pp. I148–I206.

Martinoni, D., Bernhard, L., 1998. A conceptual framework for reliable digital terrain modelling. Proceedings 8th Symposium on Spatial Data Handling, Vancouver, pp. 737–750.

Meier, M.F., Post, A., 1987. Fast tidewater glaciers. Journal of Geophysical Research 92 (B9), 9051–9058.

Mercer, J.H., 1970. Variations of some Patagonian glaciers since the Late-Glacial: II. American Journal of Science 269, 1–25.

Mercer, J.H., 1976. Glacial history of southernmost South America. Quarternary Research 6, 125–166.

Miller, A., 1976. The climate of Chile. In: Schwerdtfeger, W. (Ed.), Climates of Central and South America. World Survey of Climatology, vol. 12. Elsevier, Amsterdam, pp. 113–146.

Naruse, R., Aniya, M., Skvarca, P., Casassa, G., 1995. Recent variations of calving glaciers in Patagonia, South America, revealed by ground surveys, satellite-data analyses and numerical experiments. Annals of Glaciology 21, 297–303.

Naruse, R., Skvarca, P., Takeuchi, Y., 1997. Thinning and retreat of Glaciar Upsala, and an estimate of annual ablation changes in southern Patagonia. Annals of Glaciology 24, 38–42.

Oerlemans, J., Reichert, B.K., 2000. Relating glacier mass balance to meteorological data by using seasonal sensitivity characteristic. Journal of Glaciology 46, 1–6.

Paskoff, R., 1996. Atlas de las formas de relieve de Chile. Santiago de Chile.

Rignot, E., Rivera, A., Casassa, G., 2003. Contribution of the Patagonia Icefields of South America to sea level rise. Science 302, 434–437.

Rivera, A., Carlos, J., Casassa, G., 1997a. Recent fluctuations of glaciar Pío XI, Patagonia: Discussion of a glacial surge hypothesis. Mountain Research and Development 17, 309–322.

Rivera, A., Lange, H., Aravena, J., Casassa, G., 1997b. The 20th century advance of glaciar Pío XI, Southern Patagonia Icefield. Annals of Glaciology 24, 66–71.

Rivera, A., Casassa, G., 1999. Volume changes on Pio XI glacier, Patagonia: 1975–1995. Global and Planetary Change 22, 233–244.

Rivera, A., Acuña, C., Casassa, G., Brown, F., 2002. Use of remotely sensed and field data to estimate the contribution of Chilean glaciers to eustatic sea-level rise. Annals of Glaciology 34, 367–372.

Rosenblüth, B., Casassa, G., Fuenzalida, H., 1995. Recent climactic changes in western Patagonia. Bulletin of Glacier Research 13, 127–132.

Rosenblüth, B., Fuenzalida, H., Aceituno, P., 1997. Recent temperature variations in southern South America. International Journal of Climatology 17, 67–85.

Schneider, B., 1998. Geomorphologisch plausible Rekonstruktion der digitalen Repräsentation von Geländeoberflächen aus Höhenliniendaten. Geographisches Institut der Universität Zürich. Geoprocessing Series, vol. 35. Zürich.

Schneider, C., Glaser, M., Kilian, R., Santana, A., Butorovic, N., Casassa, G., 2003. Weather observations across the Southern Andes at 53°S. Physical Geography 24, 97–119.

Schneider, C., Kilian, R., Glaser, M., 2004. Energy balance in the ablation zone during the summer season at the Gran Campo Nevado Ice Cap in the Southern Andes. this issue.

Schnirch, M., 2001. Ableitung eines digitalen Geländemodells mit Hilfe photogrammetrischer Verfahren zur Erstellung eines

Gletscherinventars des Gran Campo Nevado, Chile. unpublished master theses, Institut für Physische Geographie, University of Freiburg, Freiburg.

Schwiedefsky, K., Ackermann, F., 1976. Photogrammetrie. Stuttgart.

Villalba, R., Lara, A., Boninsegna, J.A., Masiokas, M., Delgado, S., Aravena, J.C., Roig, F.A., Schmelter, A., Wolodarsky, A., Ripalta, A., 2003. Large-scale temperature changes across the southern Andes: 20th-century varations in the context of the past 400 years. Climatic Change 59, 177–232.

Warren, C., Aniya, M., 1999. The calving glaciers of southern South America. Global and Planetary Change 22, 59–77.

Zamora, E., Santana, A., 1979. Characteristicas climaticas de la costa occidental de la Patagonia entre las latitudes 46°40′ y 56°30′. Anales del Instituto de la Patagonia, Serie Ciencias Naturales 10, 109–143.

Zhu, H., Eastman, J.R., Schneider, K., 1999. Constrained delaunay triangulation and TIN optimization using contour data. Proceedings, Thirteenth International Conference on Applied Geologic Remote Sensing, Vancouver BC, Canada, March 1–3, 1999, pp. II-373–II-380.

Please cite this article as: Schneider, C. et al. Glacier inventory of the Gran Campo Nevado Ice Cap in the Southern Andes and glacier changes observed during recent decades. Global and Planetary Change (2006), doi:10.1016/j.gloplacha.2006.11.023